SECTION 3

OVERALL SUBASSEMBLY RESPONSE

3.1 General Response

This section describes the overall response of the slab-column connection subassemblies. The observed behavior of the subassemblies is presented in terms of load-deformation characteristics, cracking pattern, lateral load resistance, stiffness, energy dissipation capacity, and the observed mode of failure. The general behavior of the individual specimen is described first, followed by a specific discussion of response of interior and exterior connections.

SPECIMEN DNY_1: This specimen simulated the bent-up reinforcing detail in the slab and carried 30% of the uniformly distributed live load in addition to the design dead load. The slab bottom reinforcement in this detail is stopped short of the column at the interior connection. The slab top reinforcement yielded first near the face of the exterior column at 0.75% lateral drift. At 1% drift, the slab top reinforcement at interior column also yielded. The flexural cracks at the bottom of the slab at exterior connections grew to full slab width by 1.5% drift. Since only a small fraction of the slab bottom reinforcement extended into the column, yielding of the slab bottom reinforcement occurred as soon as the slab cracked under positive bending moment. Despite the limited anchorage length, the slab bottom reinforcement at the exterior column did not show any significant loss of bond or anchorage up to 2% drift. At 2.25% drift, however, the slab bottom reinforcement began to pull out of the exterior connection, resulting in a substantial increase in width of the slab bottom flexural crack. The specimen reached its peak lateral load at 3% drift. At this stage, the flexural cracks on top of the slab opened widely and the concrete along the flexural crack on the bottom surface of the slab began to crush. The slab edge developed torsional cracks adjacent to the exterior connection and the anchorage of slab reinforcement in the exterior column began to deteriorate rapidly. Response of the specimen at lower drifts was controlled by flexural yielding of the slab. Torsional cracks at the slab edge, adjacent to exterior connections, affected the response at higher drifts. By 4.5% drift, flexural-torsional cracks had fully developed at the exterior connections and flexural yield lines extended across the full width of the slab at the interior connections. After reaching the peak load at 3% drift, the lateral load resistance of the specimen dropped gradually with each additional cycle.

SPECIMEN DNY_2: Specimen DNY_2 had reinforcing detail similar to that used in specimen DNY_1 except that full dead and live load was applied to the slab during the test. The increased gravity load had a very significant effect on the failure mode of the specimen. Unlike specimen DNY_1, which predominantly experienced a flexural mode of failure, the specimen DNY_2 failed

due to punching shear at interior connection at 2% drift. The specimen sustained the first cycle at this drift level but failed in punching during the repeat cycle at the same drift value. In anticipation of this failure, special arrangement was made to contain the total collapse of the slab by placing supports a few inches clear of the slab near the interior column. The slab reinforcement at interior and exterior connections yielded early at 0.75% and 0.90% lateral drifts, respectively. The corresponding lateral load was 67% and 80% of the peak load. Because of the heavy gravity load, the flexural cracks in the connection region were visible only on the top surface of the slab adjacent to each column.

SPECIMEN DNY_3: Reinforcement in the slab of this specimen consisted of straight bars instead of the bent-up bars used in specimens DNY_1 and DNY_2. This type of reinforcing detail has also been commonly used in older flat-plate buildings. In this detail, the slab bottom bars extend into the column and the slab is expected to have more resistance to positive bending at interior connections. Since the amount of top reinforcement in the slab was the same as in the other specimens, the load at which the slab reinforcement yielded was not significantly different from the yield load of DNY_1 and DNY_2. Yielding of the slab reinforcement initiated at 1% drift and the lateral load resistance peaked at about 2% drift. At this drift level, the exterior connection region had suffered significant cracking due to shear, bending, and torsion and the behavior of the interior connection was dominated by flexural yielding of the slab. By 4.5% drift, both exterior connections had lost the ability to transfer moment between the column and the slab.

SPECIMEN DNY_4: This specimen had the same configuration and detail as the specimen DNY_1 except that an 8in.x12in. spandrel beam was added to the slab at the exterior connections. Spandrel beams have been commonly used in flat-plate buildings to support exterior walls. The presence of the spandrel beam increased the torsional stiffness of the slab edge at the exterior connection which increased the moment transfer capacity and also affected the mode of failure. Unlike the other specimens in which torsional cracks developed in the slab edge at exterior connections, a major flexural crack developed at the face of the edge beam which extended the full width of the slab. The slab reinforcement yielded first at 0.5% drift and the specimen reached its peak load at 2% drift. By 2.25% drift, the slab bottom bars extending into the spandrel beam had lost their anchorage. Although flexural yielding of the slab dominated the response for most part of the test, the interior connection appeared to punch at 4.7% drift.

3.2 Cracking Pattern

Before applying the lateral load, all specimens except DNY_2 which was subjected to full dead load plus live load were uncorked under service gravity loads (DL+0.3 LL). The application of full dead and live load to the slab in specimen DNY_2 resulted in minor flexural cracks near the interior

connection. On applying the lateral load, flexural and torsional cracks formed in the slab at exterior connections. These cracks extended and increased in width while new cracks developed at higher drift levels. The crack pattern generally stabilized by 2.5% drift. Further increase in drift only widened the existing cracks with very few new cracks.

3.3 Load-Drift Response

The observed load-drift response of the four specimens is shown in figures 3-1 through 3-4. Except for the specimen DNY_2, which was subjected to higher gravity load and thus failed early in punching shear, the load-drift response of the specimens generally appears to be very similar. The envelope of the hysteresis loops in each loading direction is approximately bilinear with some tendency of gradual strength reduction beyond the peak load. Since the slab reinforcement yields in a progressive manner, the yield point is not very well defined. The loops are severely pinched, indicating a rapid loss of stiffness and a low energy dissipation capacity. In specimens with dominant flexural yield lines, energy was dissipated mostly by yielding of the slab reinforcement and opening of the flexural cracks. Slippage of the reinforcing bars, local crushing of concrete, and friction along the major cracks also contributed to dissipation of energy. The load-deformation response generally resembled that of an under reinforced flexural member with the exception of a well-defined yield point. Specimen DNY_3 experienced an unexpected initial large displacement of 1.5% drift due to a malfunction in the servo-control mechanism which resulted in lower stiffness of the specimen during the regular test cycles. The specimen DNY_2, because of the higher gravity load, sustained only a limited number of cycles suggesting reduction in deformation capacity under increased gravity load.

3.4 Strength

The overall lateral load resistance of the specimens depended very much on the performance of slab-column connections. When the connection failed prematurely in punching shear, as in specimen DNY_2, the slab could not develop its full flexural capacity and the observed strength of the specimen was lower. The specimens DNY_1, DNY_3, and DNY_4, which resisted the lateral load primarily through bending of the slab, were able to develop their full strength and sustained that load for at least upto 3% drift despite the loss of anchorage of the slab bottom bars at exterior connections.

The peak load and corresponding drift of specimens are given in table 3-I and the envelope of load-drift loops is shown in figure 3-5. The slab reinforcement typically yielded first at exterior connections except in DNY_2 where the slab first yielded at the interior connection. Because of the presence of the spandrel beam at exterior connection, the slab reinforcement yielded early at 0.5% drift in DNY_4. The peak loads in the positive loading direction were within 10% of the average peak

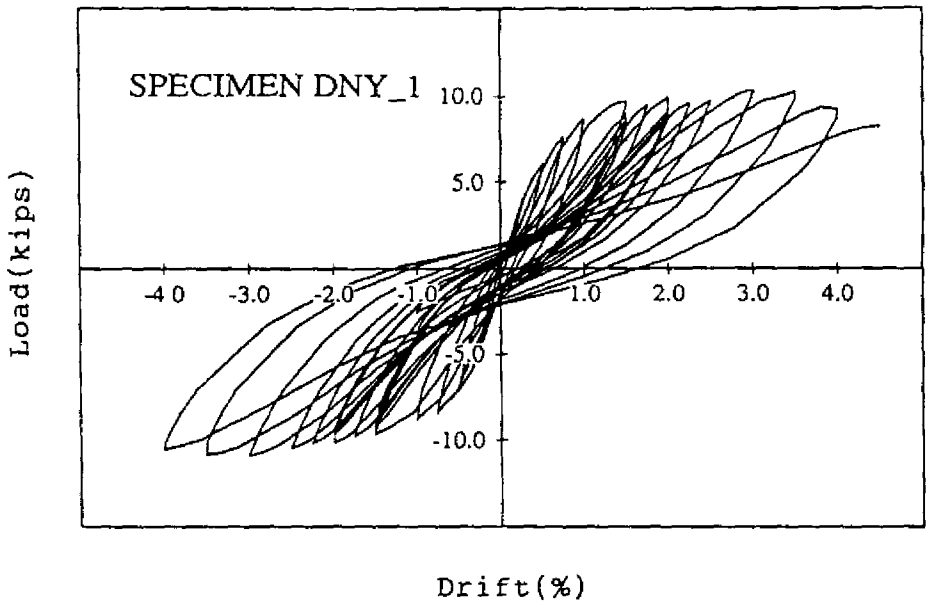

FIGURE 3-1 Hysteresis Loops of DNY_1

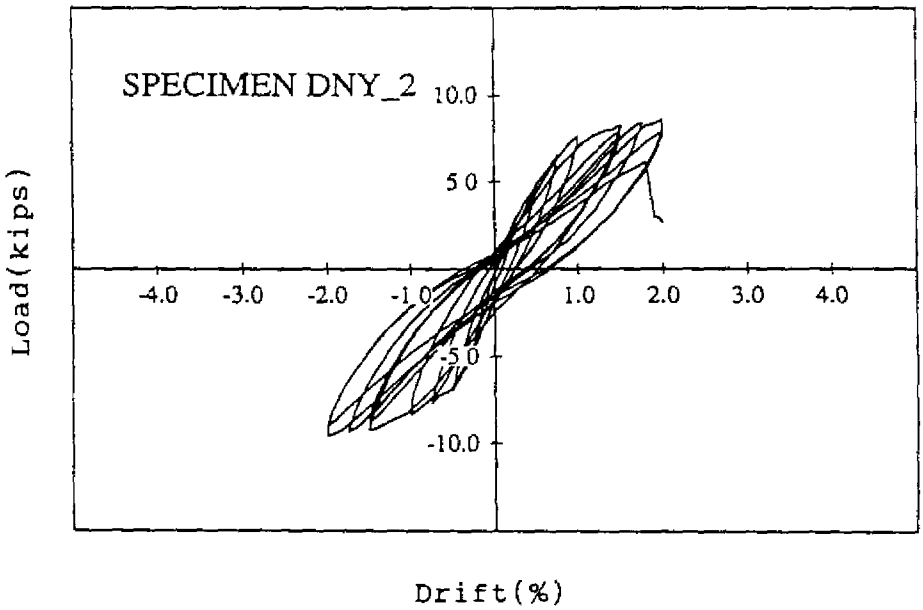

FIGURE 3-2 Hysteresis Loops of DNY_2

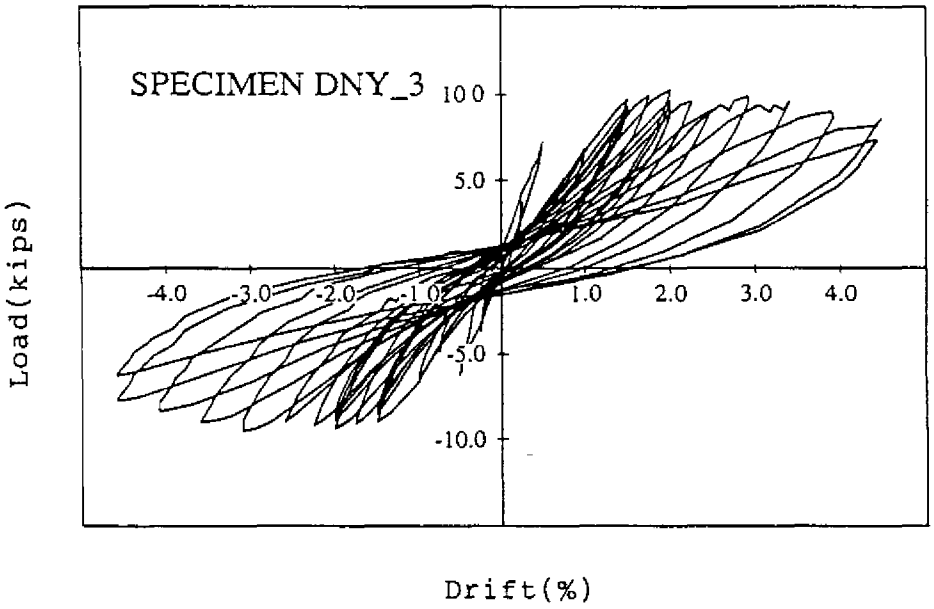

FIGURE 3-3 Hysteresis Loops of DNY_3

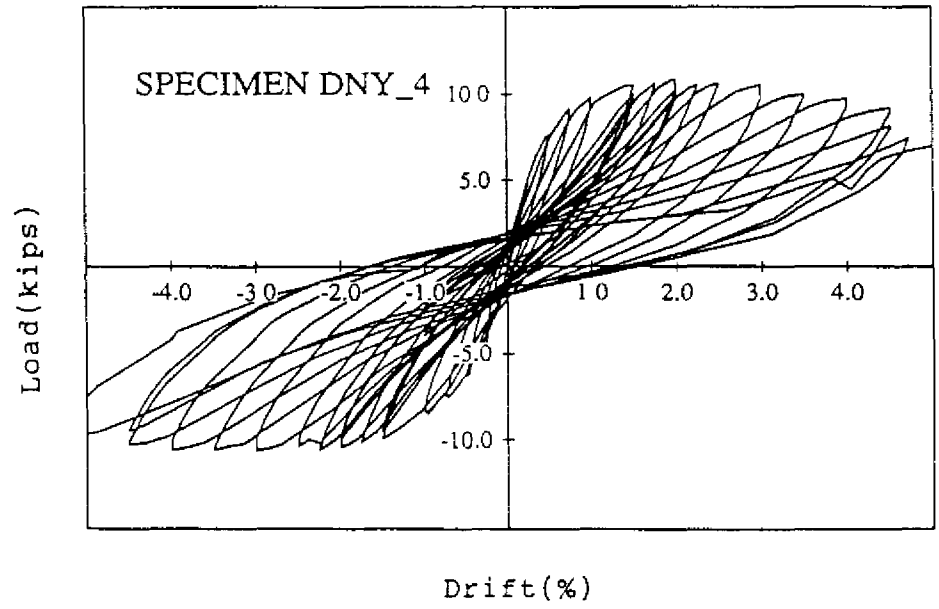

FIGURE 3-4 Hysteresis Loops of DNY_4

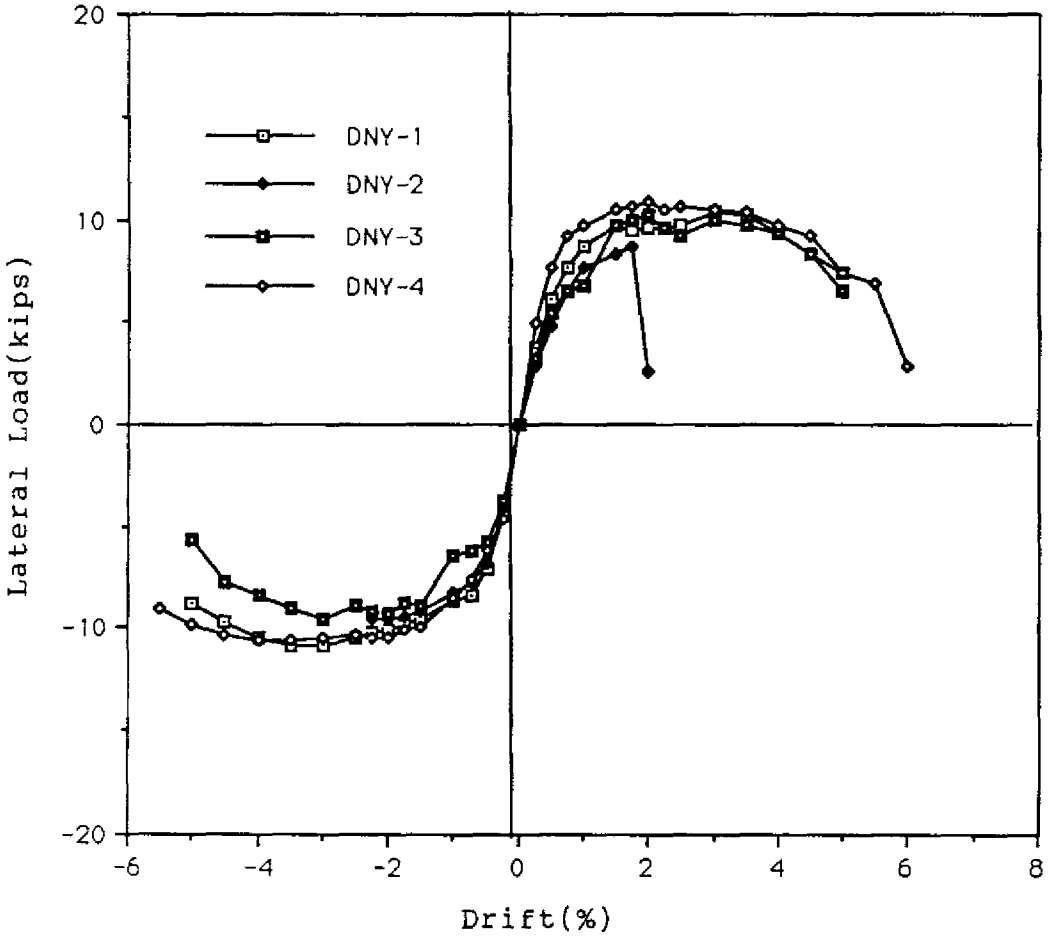

FIGURE 3-5 Load-Deformation Envelope of Specimens

load of 10.4 kips. The average peak load in the negative direction was approximately 5% smaller than the average peak load reached in the positive direction.The specimens DNY_2 and DNY_4 lost their strength when interior connections failed in punching.

The loss of strength under repeat cycles was evaluated by repeating load cycles at 1.5, 2.0 and 4.5% drifts. Before reaching the peak load, the reduction in strength during the first repeat cycle was 5 to 8% and during the third repeat cycle the drop in strength was 7 to 11%. However, after the peak load, the reduction in strength increased to 10 to 18%. Typical loops from repeat cycles are shown in figure 3-6. Several small displacement cycles of 1% drift were repeated at predefined intervals to evaluate the low amplitude stiffness degradation and the loss of energy dissipation capacity of the specimens. A typical comparison between the two loops, one at initial 1% drift and the other at 1% drift following the 2% drift cycle, is shown in figure 3-7. Both the energy dissipation capacity and the lateral load resistance during the second small drift cycle are significantly smaller.

TABLE 3-I Ultimate Response and Failure Mode of Specimens

Specimen	Peak Load (kips)	Peak Drift (%)	Ultimate Load (kips)	Ultimate Drift (%)	Failure Mode
DNY_1	10.9	3.0	8.7	4.5	Flexure
DNY_2	9.6	2.0	7.7	2.0	Punching
DNY_3	10.2	2.0	8.2	4.5	Flexure
DNY_4	10.9	2.6	8.7	4.7	Punching

3.5 Stiffness

Flat-plate connections are inherently flexible and their stiffness rapidly degrades under cyclic loading. The observed stiffness degradation of the subassemblies during the positive and negative loading directions is shown in figure 3-8. For simplicity, the stiffness here is defined as slope of the line connecting origin to the peak displacement point during a given half-cycle. The initial stiffness and the change in stiffness varied among the specimens upto 2% drift. Beyond this drift level, the stiffness of all specimens was very similar and it also degraded in an identical manner. The specimen DNY_2, which was subjected to a higher gravity load, had the least initial stiffness compared to the other specimens. This is attributed to initial cracking of the slab under increased gravity load. The specimen with the edge beam had the highest initial stiffness in both positive and negative loading directions due to the restraining effect of the spandrel beam. Different slab reinforcing detail in specimens DNY_1 and DNY_3 did not have significant effect on their stiffness. The stiff-

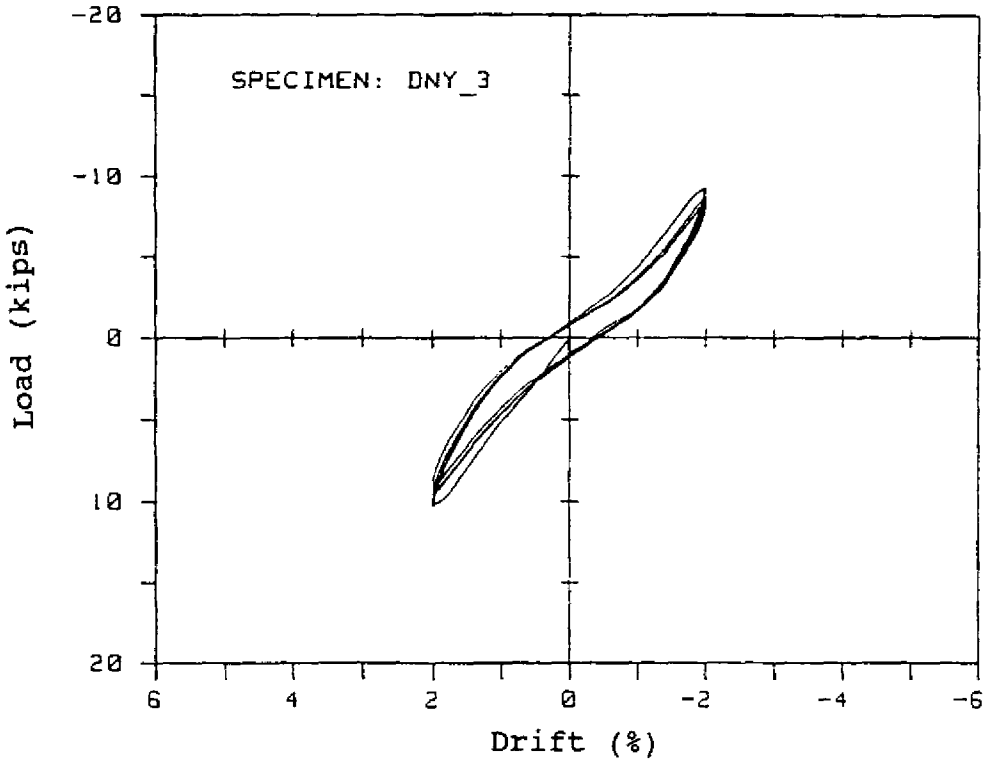

FIGURE 3-6 Load vs. Drift Response Under Repeated Cycles

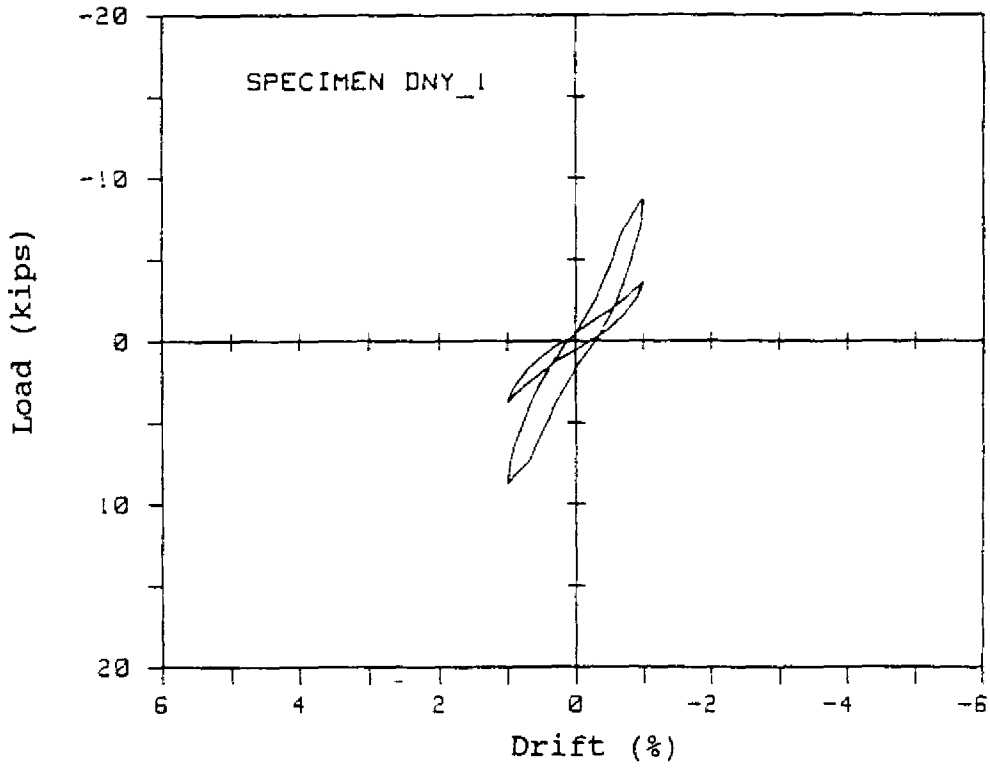

FIGURE 3-7 Comparison of Displacement Cycles

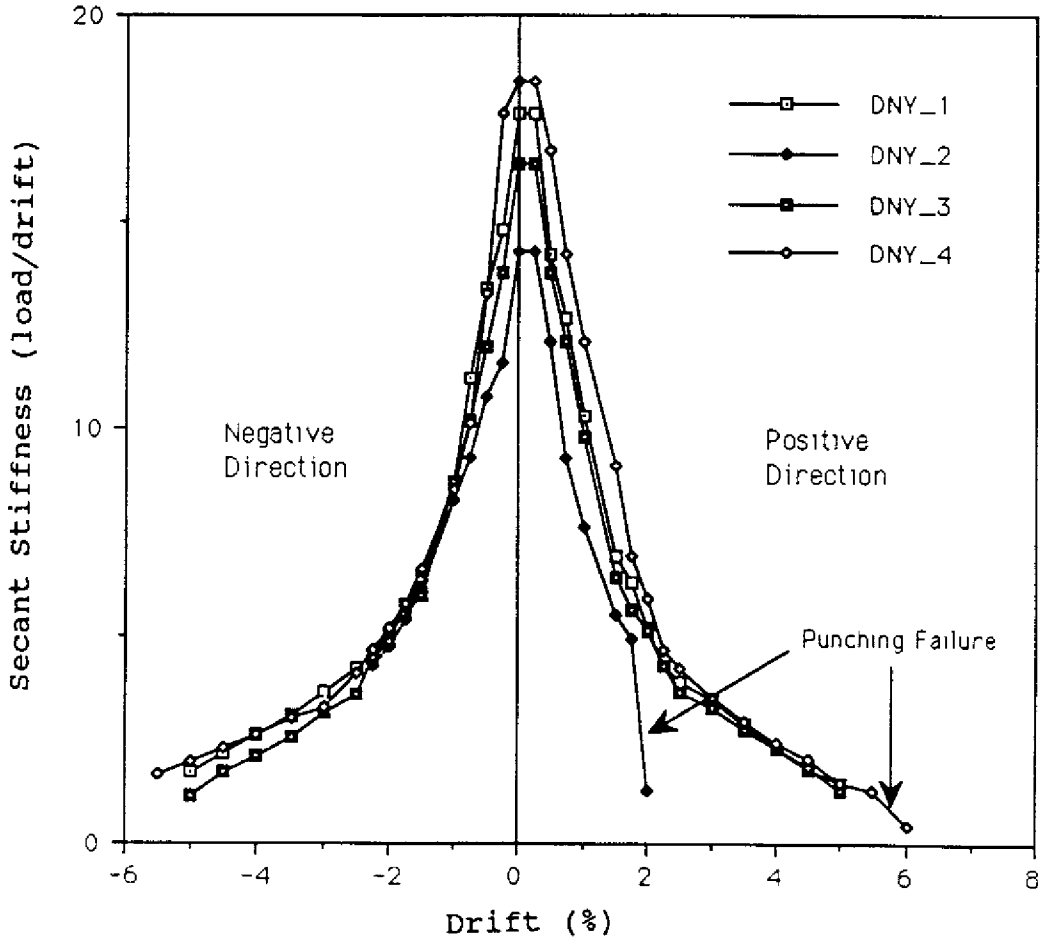

FIGURE 3-8 Stiffness Degradation of Specimens

ness during the negative half-cycle was in general slightly lower than the stiffness during the positive half-cycle. Approximately 50% of the initial stiffness was lost during the first 1% drift. Additional 20% was lost when the specimens reached two% drift. Only 10% of the initial stiffness remained by the time the specimens reached 5% lateral drift.

3.6 Ductility

Deformation capacity of connections has been traditionally expressed in the form of a ductility factor which is usually defined as a ratio of ultimate displacement to displacement at first yield of reinforcement. The slab-column connections, however, do not exhibit a well defined yield point. A common definition of yield point is illustrated in figure 3-9. In this definition, the intersection of a secant line connecting the origin with 75% of the peak load on the primary curve and the horizontal line through the peak load is assumed as the yield point. If a 20% loss of strength is assumed acceptable, then the ultimate displacement can be determined corresponding to 80% residual strength. Table 3-II shows the dactylitis of the subassemblies based on this definition. The specimen DNY_4 with the edge beam had the largest ductility of 5.9, and the specimen DNY_2 with highest gravity load had the least ductility of 2.0. The reinforcing detail in the slab appears to have some effect on the ductility of the specimens. The specimen with the bent-up slab reinforcement had a ductility of 4.3 while the specimen with straight bars in the slab showed a ductility of 3.75. The difference in deformation capacity of the two specimens is attributed to different anchorage detail of the slab bottom reinforcement

TABLE 3-II Ductility of Specimens

Specimen	Interior Connection		Exterior Connection		Subassembly Response			
	P_y	D_y	P_y	D_y	P_y (kips)	D_y^* (%)	D_u (%)	D_u/D_y
DNY_1	8.74	1.05	8.33	0.75	8.21	1.05	4.50	4.28
DNY_2	6.48	0.77	7.69	0.88	7.23	1.00	2.00	2.00
DNY_3	6.46	0.96	7.96	1.00	7.50	1.20	4.50	3.75
DNY_4	9.23	0.78	6.25	0.50	8.23	0.80	4.70	5.88

*. Based on assumed yield value

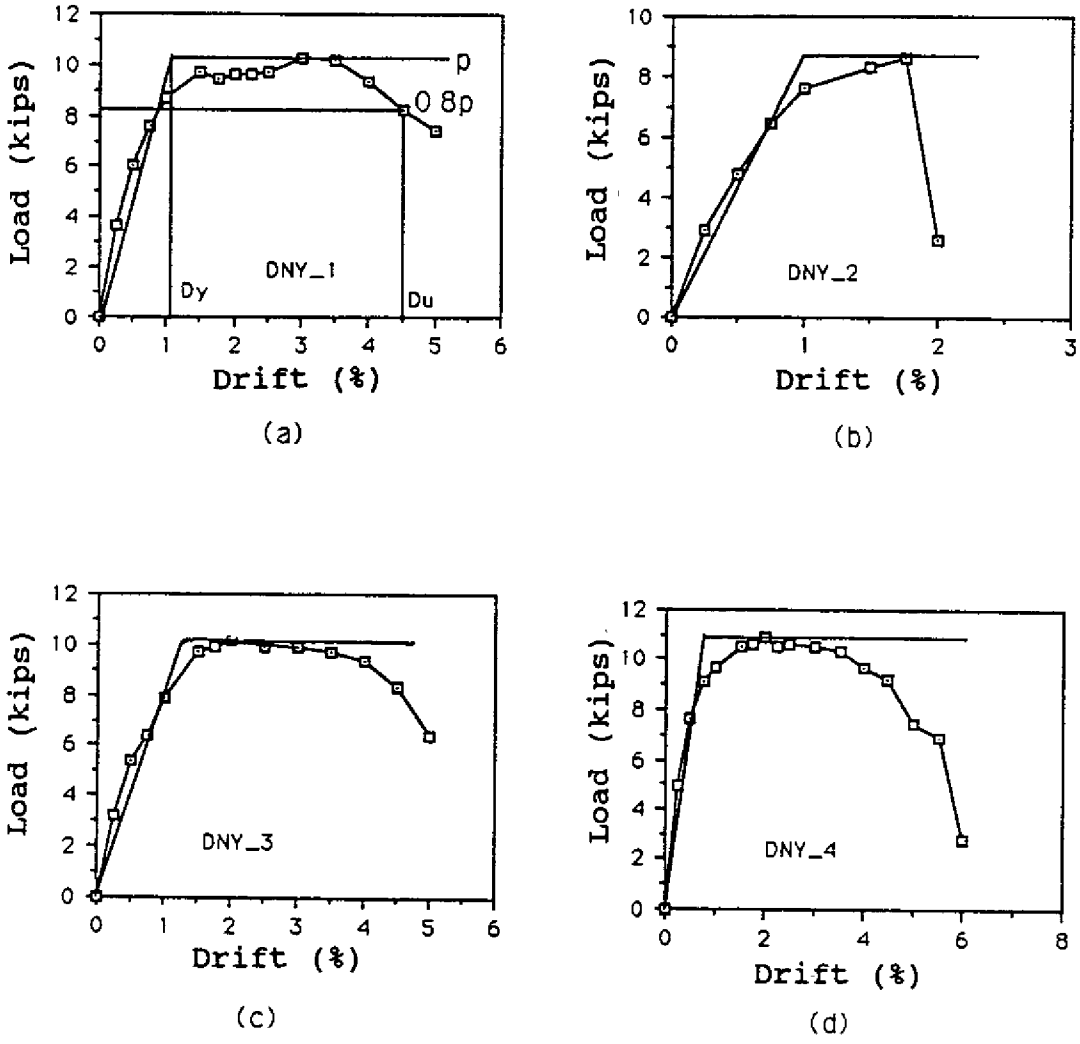

FIGURE 3-9 Ductility of Specimens

3.7 Anchorage Performance

At interior connections, the slab bottom reinforcement either extended a limited distance into the interior column or stopped short of the column depending upon whether straight or bent-up reinforcing detail was used. At exterior connections, the slab bottom reinforcement continued into the column a distance of six inches. However, the amount of slab bottom reinforcement continuing into the column is so small that under reversal of loading, it would yield as soon as the slab reached its cracking moment. The ability to transfer moment between the slab and the column under positive bending, therefore, depended much on the anchorage performance. The slab bottom reinforcement lost its anchorage at exterior connections soon after yielding under positive bending. Until that point, the slab bottom reinforcement assisted in limiting the width of slab flexural cracks. However, once the anchorage failed, the moment-transfer capacity under positive bending became negligible and the lateral load capacity dropped followed immediately by redistribution of the load to other columns. The effect of a local anchorage failure at a connection did not appear to have a dramatic effect on the overall response of the subassembly. After the loss of anchorage, the lateral load was resisted by the connections with slab under negative bending. Specific detail of the anchorage performance will be presented later when the behavior of individual connections is discussed.

3.8 Moment Redistribution

Moment distribution in the slab along the column line explains both the cracking pattern and the interaction among the different connections. Slab reinforcing detail, the presence of a spandrel beam, and intensity of the gravity load all affected the distribution of moment in the slab. The ultimate shape of the moment diagram is influenced by the changes in stiffness of the individual connections and their failure modes. The discussion below will focus on several aspects of moment redistribution among connections.

The two levels of gravity load in combination with the lateral load produced two distinct responses. The gravity load dominated the response under full dead and live loads and the lateral load dominated the response under the service loads. Figure 3.10 shows the observed distribution of moment for the two cases. The moment diagrams due to gravity load alone are shown in figures 3-10 (a) and 3-10 (b). Under gravity loads only, the slab mostly remained elastic and the negative moment at interior connections was approximately three times larger than the negative moment at exterior connections. Also, one-half of the total gravity load was carried by the interior column. The combined gravity and lateral load moment diagram for DNY_1 at 2.0% drift is shown in figure3-10(c). After several load reversals, the negative moments at exterior connections due to gravity load alone became significantly smaller. Furthermore, distribution of the lateral load among the three columns changed considerably with the interior column resisting 65% of the lateral load at 2% drift.

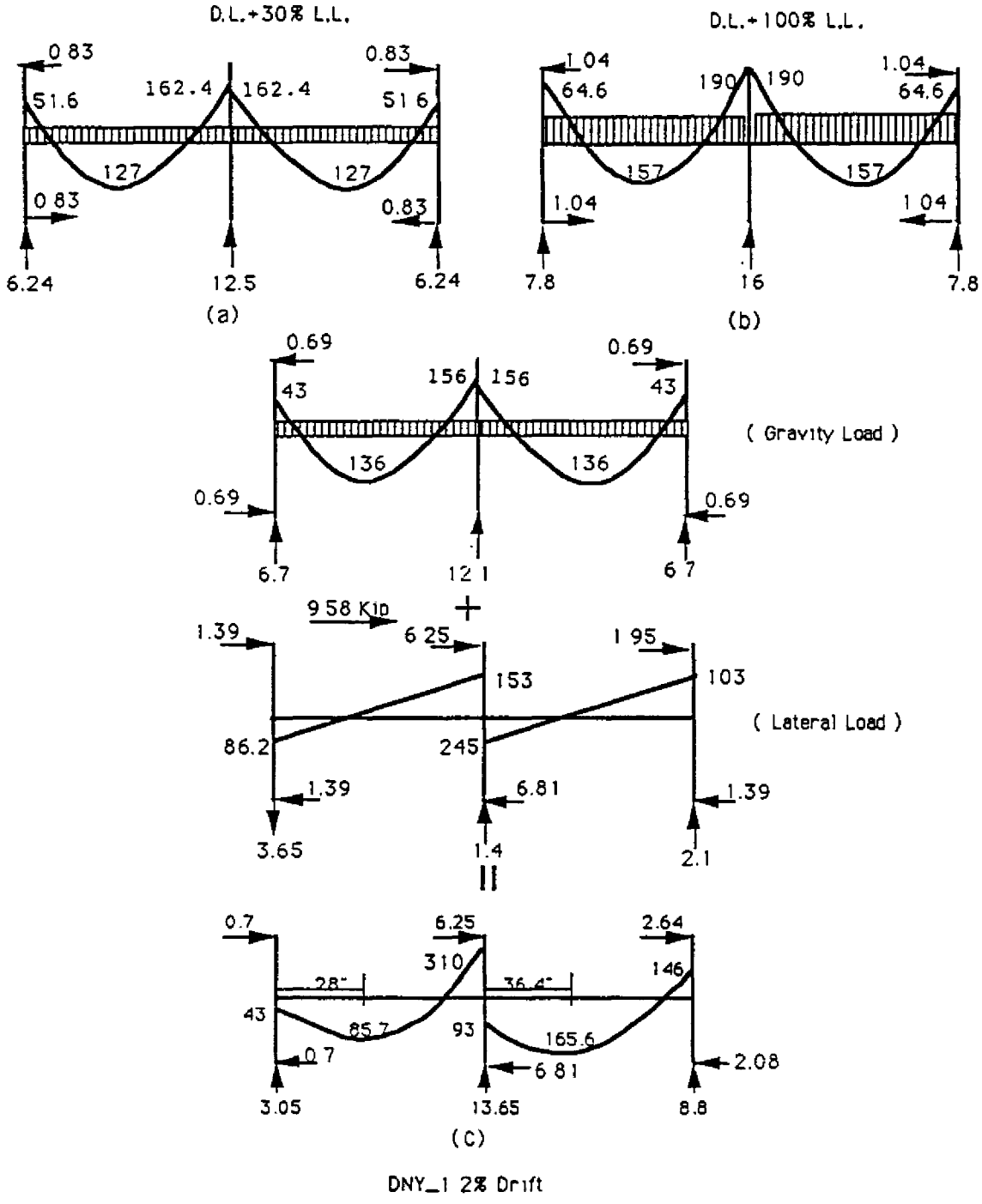

FIGURE 3-10 Observed Moment Distribution in DNY_1 and DNY_2

The effect of drift level on the distribution of moment in DNY_1 is shown in figures 3-11(a) and 3-11(b). At 0.5% drift, the response was essentially elastic. Forty two percent of the lateral load was carried by the interior column and the rest resisted by the exterior columns. The maximum positive moment was near the center of each span. As the drift level increased, the positive moments near the column exceeded the cracking strength of the slab. By 2% drift, the slab top reinforcement near the columns had yielded and the subassembly reached its maximum lateral resistance. The moment diagram at this stage reflects the effect of cracking in the slab under reversed loading and yielding of the slab top reinforcement. As soon as the slab at left exterior connection reached its cracking strength in positive bending, the moment carried by the left exterior connection decreased considerably and it redistributed to the interior connection on the column side with slab top reinforcement in tension. Early loss of stiffness at the exterior connections transferred a significant portion of the gravity and lateral load to the interior connection. At 2% drift, the interior connection carried 65% of the lateral load while the left exterior connection carried only 7.5% of the lateral load. The positive moment at the face of the interior column was always below the cracking moment due to the presence of the gravity load. The flexural cracks in the bottom of the slab in the right span were therefore closer to the mid-span where the moment exceeded the cracking strength.

The effect of higher gravity load on moment distribution at 2% drift is illustrated in figure 3-11(c). Since the specimen DNY_2 experienced full dead and live load, the interior connection was subjected to high shear. A few interesting observations can be made from the moment response of this subassembly: (1) gravity load dominated the response and caused early cracking of the slab on top near the connections, (2) the maximum positive moment occurred was closer to the mid-span, (3) because of the high initial negative moments in the connection regions, the cracking of the slab under positive moment could only occur a certain distance away from the column face. At 2% drift, the moment at exterior connections were thus smaller than the moment at the interior connection. Approximately, 59% of the lateral load was carried by the interior column and the remaining was equally shared by exterior columns.

The effect of loss of anchorage on the distribution of moments can been seen in figure 3-11(d) which shows the observed moments in specimen DNY_3 at 3% drift. The loss of anchorage of slab bottom reinforcement at left exterior connection significantly reduced the moment transfer capacity of the connection with lateral load redistributing to the interior connection. At this drift level, the edge connection acted more like a hinge support and the maximum positive moment in the left span was only 62% of the cracking strength of the slab at midspan. The cracking moment in the right span occurred approximately 7 in. from the face of the interior column.

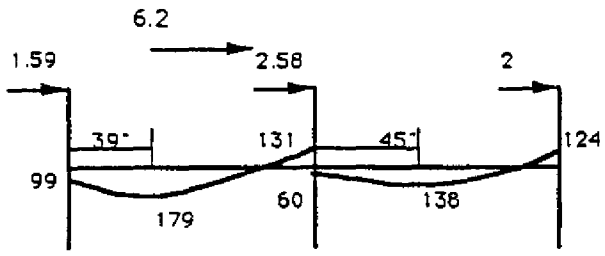

(a) DNY-1 at 0.5% Drift

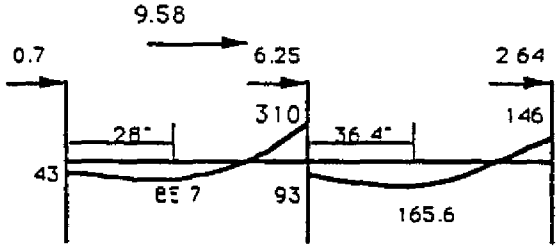

(b) DNY-1 at 2% Drift

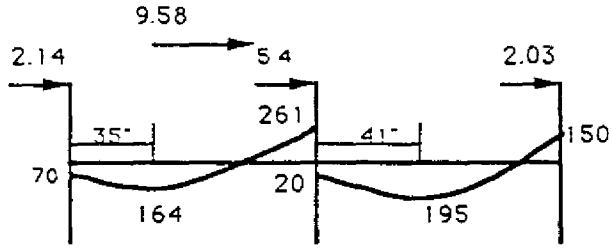

(c) DNY-2 at 2% Drift

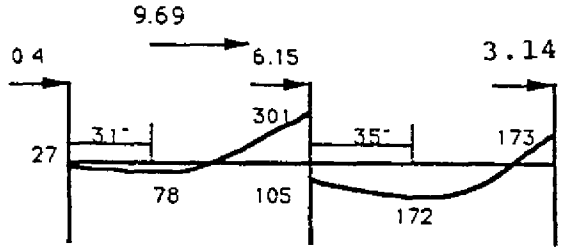

(d) DNY-3 at 3% Drift

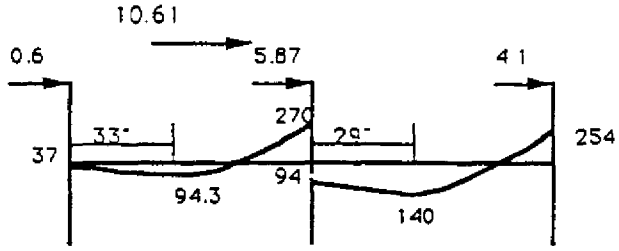

(e) DNY-4 at 2% Drift

FIGURE 3-11 Observed Lateral Force Distribution in Specimens

The presence of a spandrel beam greatly improved the negative moment-transfer capacity at the exterior connections. However, the positive moment transfer at exterior connection was not affected by the presence of the spandrel beam as illustrated in figure3-11 (e).

3.9 Deflection of Slab

The deflection of slab due to lateral and gravity loads was measured during each test. These deflections were measured 8 in. and 24 in. away from the column line. The effect of initial gravity load on the deflected shape of the slab can be seen by comparing the slab deflections of specimens DNY_1 and DNY_2 at 2% drift as shown in figure 3-12. The specimen DNY_1, which carried full dead load plus 30% of the live load, had an antisymmetric deformed shape indicating a dominating effect of the lateral load. The point of contraflexure was close to the midspan and the deflections were relatively small. By increasing the gravity load to full dead and live load, the inflection point disappeared from the right span and it moved closer to the interior connection in the left span. The exterior connections at 2% drift acted more like hinged supports. The moment transfer at the interior connection occurred only on the side of the column with slab top in tension as indicated by negative deflection of the slab. The maximum deflection in DNY_2 was almost six times the deflection observed in DNY_1. The initial cracking of the slab due to heavier gravity load appears to have a very significant effect on the deformed shape of the slab.

Figure 3.13 compares the deformed shape of the slab of specimen DNY_2 at 0% and 2% drifts. The effect of initial cracking in the slab at the interior connection and resulting initial deflections are to be noted. Lateral load increased the deflection in the first span along the loading direction and reduced the deflection in the second span, but the effect was not very significant. The gravity load expectedly controlled the response of this specimen.

The presence of spandrel beam in specimen DNY_4 attracted more moment at the exterior connections which affected the deformed shape of the slab. As shown in figure3.14, larger deflection change occurred near the exterior connections. Because of the restraining effect of the spandrel beam, the deflection and rotation of the slab at interior connection of DNY_4 was smaller than those in DNY_1 on both sides of the column.

The effect of anchorage loss and larger effective slab width due to the presence of spandrel beam can be seen by comparing the deflected shape of specimens DNY_3 and DNY_4 at 4% drift as shown in figure 3-15. The loss of anchorage of slab bottom reinforcement at the right exterior connections of the two specimens resulted in a very similar deflected shape. However, since a larger slab width participated at the edge connection of DNY_4 due to the presence of the spandrel beam, the rotation and deflection of the slab left edge was smaller compared to that observed in DNY_3.

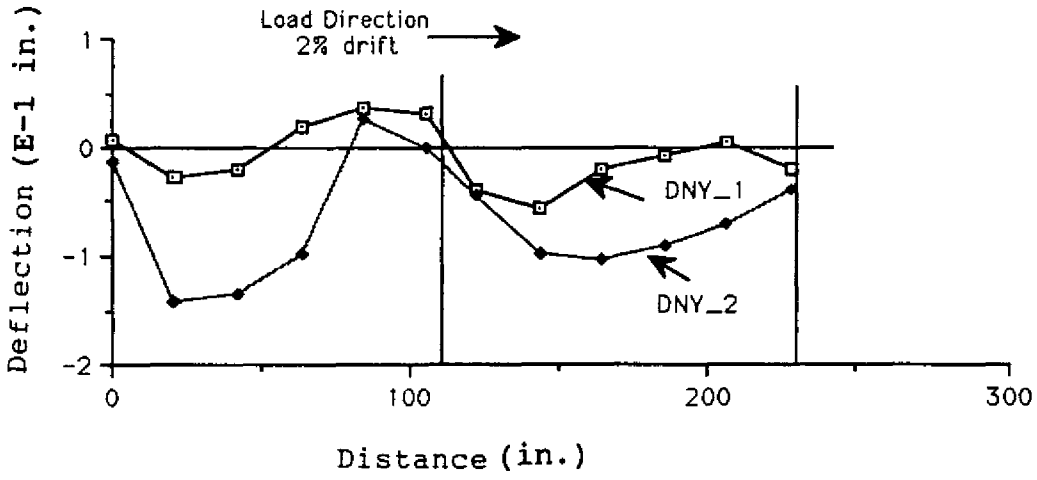

FIGURE 3-12 Effect of Gravity Load on Slab Deflection

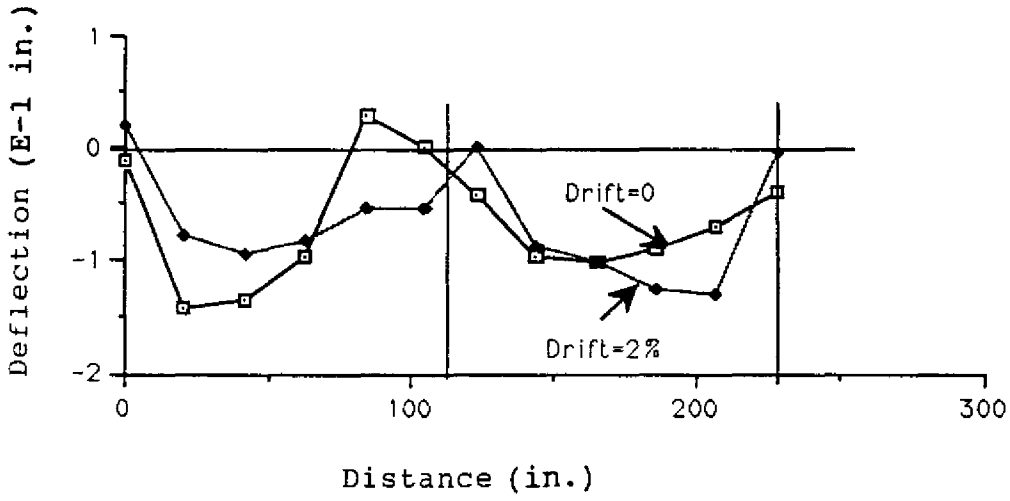

FIGURE 3-13 Slab Deflection Due to Lateral Load

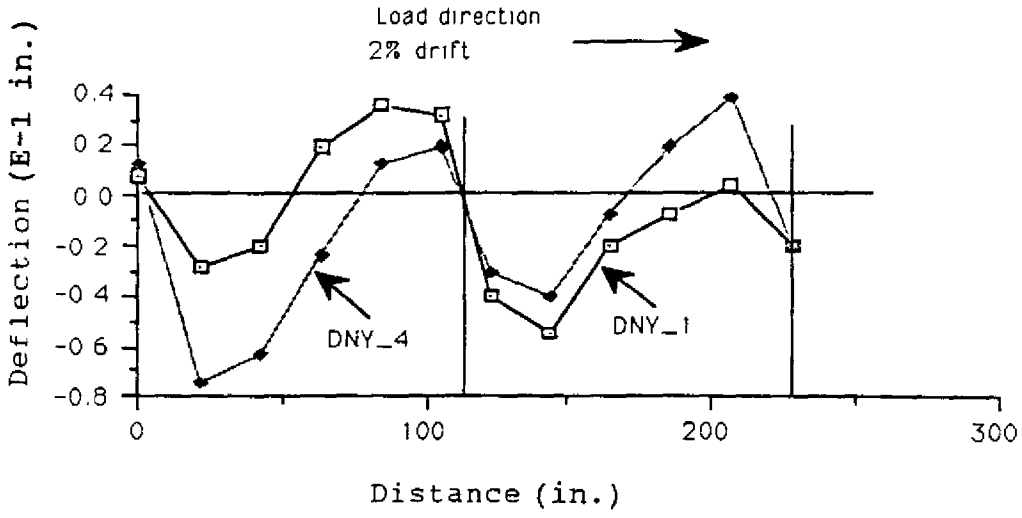

FIGURE 3-14 Effect of Spandrel Beam on Slab Deflection

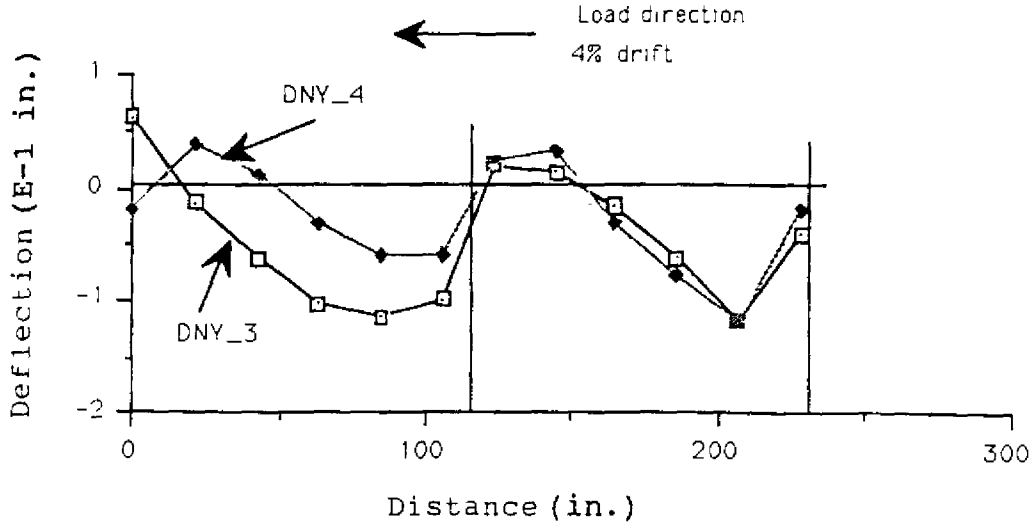

FIGURE 3-15 Comparison of Slab Deflection in DNY_3 and DNY_4